Different Approaches of PID Control UAV Type Quadrotor

G. Szafranski, R. Czyba
Silesian University of Technology, Akademicka St 16, Gliwice, Poland

http://www.imavs.org/

ABSTRACT

In this paper we focus on the different control strategies for the unmanned aerial vehicles (UAV). The control task is formulated as an angular stabilization of the quadrotor platform, and also as a tracking problem of chosen state variables. The PID algorithm has been considered in three structures in respect of the optimal control signal applied to the actuators. For better performance of quadrotor during the hover mode the cascade control system has been proposed.

The experiment results for the platform orientation control with different PID controller architectures are presented, and confirm the effectiveness of the proposed method and theoretical expectations.

1 INTRODUCTION

Unmanned aerial platforms are not a new invention. They were first introduced during the World War I, but not until recently have been flown autonomously. Among the several kinds of mini and micro unmanned aerial vehicles (MUAVs), quadrotors are probably the most common. This platform can occur in one of two configurations, ”plus” or ”cross” shape, and has been widely developed by many Universities such as MIT or Stanford/Berkeley, and commercial companies Draganflyer, X3D-BL, Xaircraft [6]. The great maneuverability and possible small size of this platform make it suitable for indoor use, as well as for outdoor applications. Such aerial platform has several application domains [4], [7]: safety, natural risk management, environmental protection, management of the large infrastructures, agriculture and film production. This aerial vehicle is highly maneuverable, has the potential to hover and to take-off, fly, and land in small areas, and has a simple control mechanism. However, a quadrotor is unstable and impossible to fly in full open loop system. The dynamics of a flying vehicle is more complex than the ground robots, so that even the hovering becomes a non-trivial task. Thus, control of a nonlinear plant is a problem of both practical and theoretical interest.

Improved performance expected from the new generation of VTOL vehicles is possible through derivation and implementation of specific control techniques incorporating limitations related to sensors and actuators. The well-known approach to decoupling problem solution based on the Non-linear Inverse Dynamics (NID) method may be used if the parameters of the plant model and external disturbances are exactly known. Usually, incomplete information about systems in real practical tasks take place. In this case adaptive control methods or control systems with sliding mode [3], [4] may be used for solving such control problem.

Email address: grzegorz.szafranski@polsl.pl, roman.czyba@polsl.pl.

A way of the algorithmic solution of this problem under condition of incomplete information about varying parameters of the plant and unknown external disturbances is the application of the Dynamic Contraction Method (DCM) [14] applied in [10]. But the most problems of those approaches in real applications are: high order of the controller equations and influence of measurement noise for a control quality. Approximations of higher derivatives amplify the measurement noise and cause abrupt changes of control signal. Therefore in this paper the different structures of PID controllers, which can reduced the adverse effects are considered.

The main aim of this research effort is to examine the effectiveness of a designed attitude control system for the quadrotor in the cascade control system with different types of PID controllers [2],[5].

The paper is organized as follows. First, a mathematical description of the quadrotor nonlinear model is introduced. The next part presents a general structure of a cascade control system, and investigation of three types of PID controllers with modified loop structure. This section includes the schemes and description of PID controller type A, B, C. The next chapter shows the results of simulations in two sections: first – inner loop control with all types PID controllers; second – performed in the cascade control system. Finally, the conclusions are briefly discussed in the last chapter.

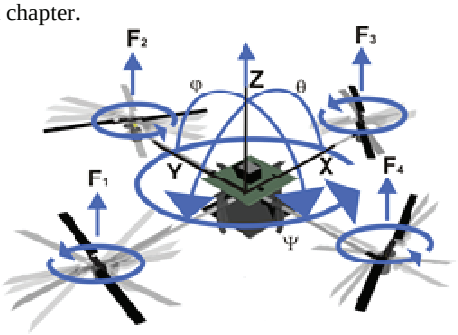

Figure 1: Quad-thrust aerial vehicle.

2 QUADROTOR MODEL

Described below the quadrotor model based on the self-modified version of a commercial Draganflyer platform. The aerial vehicle consists of a rigid cross frame equipped with four rotors as shown in Fig. 1.

The two pairs of propellers (1,3) and (2,4) turn in opposite directions. By varying the rotor speed, one can change the lift force and create motion. Thus, increasing or decreasing the four propeller’s speeds together generates vertical motion. Changing the 2 and 4 propeller’s speed conversely produces roll rotation coupled with lateral motion. Pitch rotation and the longitudinal motion result

from 1 and 3 propeller's speed conversely modified. Yaw rotation – as a result from the difference in the counter-torque between each pair of propellers [8].

2.1 Rigid Body Model

The quadrotor is a six degrees of freedom system defined with twelve states. The following state and control vectors are adopted:

(1) $X = \left[\ ,\ ,\ ,\ ,\ ,\ ,x,\dot{x},y,\dot{y},z,\dot{z}\right]^T$

(2) $U = \left[u_1,u_2,u_3,u_4\right]^T$

where: u_i - control input of motor,
$i = 1,2,3,4$ - motor number.

Six out of twelve states govern the attitude of the system (Fig.2). These include the Euler angles (, ,) and angular rates around the three orthogonal body axes. The other six states determine the position (x, y, z) and linear velocities of the center of mass of the quadrotor with respect to a fixed reference frame.

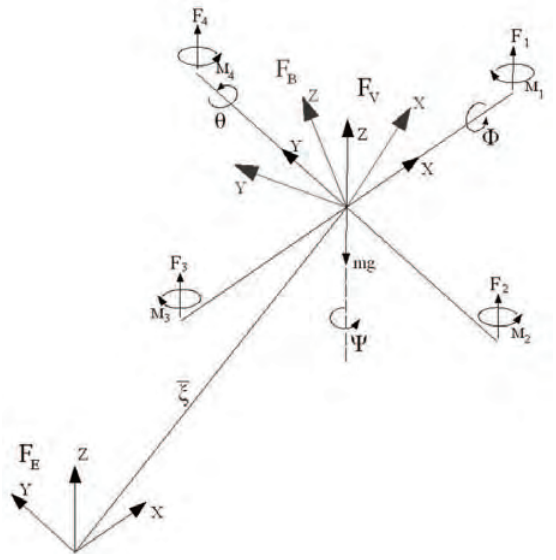

Figure 2: Quad-thrust aerial vehicle.

Using the Lagrangian, and the general form of the equations of motion in Lagrange method [1], [8], [12], [13]:

(3) $L = T_K - V$

(4) $F = \dfrac{d}{dt}\left(\dfrac{\partial L}{\partial \dot{q}}\right) - \dfrac{\partial L}{\partial q}$

where: L is Lagrangian, T_K is kinetic energy, V is potential energy, $q = \left[x, y, z, \ ,\ ,\ \right]^T$ is a vector of generalized coordinates, $F = \left(F_E, T\right)$ are a generalized forces F_E and moments T applied to the quadrotor due to the control inputs.

For translational motion the Lagrange equation has a form:

(5) $F_E = \dfrac{d}{dt}\left(\dfrac{\partial L}{\partial \dot{}}\right) - \dfrac{\partial L}{\partial}$

where: $= \left[x, y, z\right]^T$ - position coordinates,

$$F_E = \begin{bmatrix} \sin(\ ) \\ -\sin(\ )\cos(\ ) \\ \cos(\ )\cos(\ ) \end{bmatrix} \cdot f_g$$

$f_g = F_1 + F_2 + F_3 + F_4$

$F_i = b\Omega_i^2$

Ω_i - rotor speed

b - thrust factor

Accordingly, the Lagrange equation for rotary motion is following:

(6) $T = \dfrac{d}{dt}\left(\dfrac{\partial L}{\partial \dot{}}\right) - \dfrac{\partial L}{\partial}$

where:

$= \left[\ ,\ ,\ \right]^T$ - Euler angles

$T = \left[T \quad T \quad T\ \right]^T$

$T\ = bl\left(\Omega_4^2 - \Omega_2^2\right) - J_r\,\dot{}\left(\Omega_1 + \Omega_3 - \Omega_2 - \Omega_4\right)$

$T\ = bl\left(\Omega_3^2 - \Omega_1^2\right) + J_r\,\dot{}\left(\Omega_1 + \Omega_3 - \Omega_2 - \Omega_4\right)$

$T\ = d\left(\Omega_1^2 - \Omega_2^2 + \Omega_3^2 - \Omega_4^2\right)$

l - distance between propeller center and CoG

J_r - rotor inertia

d - drag factor

Above torques equations (T ,T ,T) consist of the action of the thrust forces difference of each pair, and from the gyroscopic effect.

Finally the quadrotor dynamic model with x, y, z, motions as a consequence of a pitch, roll and yaw rotations is as follows:

(7) $\ddot{} = \dfrac{1}{I_{xx}}\left(-\dot{}^2\left(I_{xx} - I_{zz}\right)s(\ )c(\ ) - \dot{}\,\dot{}\,I_{zz}c(\ ) + T\right)$

(8) $\ddot{} = \dfrac{1}{I_{yy}\left(1 + s^2(\ )\right)}\left(-\ddot{}\,I_{zz}s(\ ) - \dot{}\,\dot{}\,c(\ )s(\ )\cdot\right.$
$\left.\cdot\left(2I_{zz} - 2I_{yy}\right) - \dot{}\,\dot{}\,I_{zz}c(\ ) + T\right)$

(9) $\ddot{} = \dfrac{1}{I_{zz}}\left(-\ddot{}\,I_{zz}s(\ ) + T\right)$

(10) $\ddot{x} = \dfrac{f_g}{m}s(\ )$

(11) $\ddot{y} = -\dfrac{f_g}{m}c(\ )s(\ )$

(12) $\ddot{z} = \dfrac{f_g}{m}c(\ )c(\ ) - g$

where:

s and c are abbreviations of '*sin*' and '*cos*',

I_{xx}, I_{yy}, I_{zz} - inertia moments.

http://www.imavs.org/

http://www.imavs.org/

2.2 Propulsion system

The dynamics of the propulsion system consists of a DC motor and propeller. Motor model can be considered as a first order differential equation (13) because of a very low inductance.

$$J_r \frac{d\Omega_m}{dt} = \frac{k_m}{R} u - \frac{k_m k_e}{R} \Omega_m - \quad _l \tag{13}$$

where: u - motor input, R - motor resistance, k_e - motor electrical constant, Ω_m - motor angular speed, J_r - rotor inertia, k_m - torque constant, $_l$ - motor load.

The torque produced by motor is converted by propeller to the thrust force [9], [11]. The relationship between the angular velocity and the thrust is given in the following form:

$$F_T = C_T \quad D^4 \cdot n_P^2 \tag{14}$$

The thrust coefficient C_T is a propeller parameter and it primarily depends on the λ ratio given as:

$$= \frac{V}{n_p D} \tag{15}$$

where: V – air speed, n_p – propeller velocity in revolutions per second, D – propeller diameter, ρ is the air density.

Finally we obtain propulsion system modeled as a series connection of a linear first order dynamic element and static nonlinear second degree polynomial (Fig. 3).

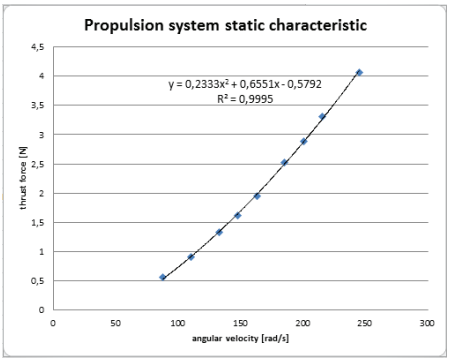

Figure 3: Static characteristic of propulsion system.

3 CONTROL SCHEME

In control applications, the rejection of external disturbances and performance improvement is a major concern. In order to fulfill such requirements, the implementation of a cascade control system can be considered. Basically, in a cascade control schema the plant has one input and two or more outputs [2]. Indeed, this requires an additional sensor to be employed so that the fast dynamics could be measured.

The primary controller and the primary dynamics are components of the outer loop. The inner loop is also a part of the outer loop, since the primary controller calculates the set point for the secondary controller loop. Furthermore the inner loop represents the fast dynamics, whereas the outer should be significantly slower (with respect to the inner loop). This assumption allows to restrain interaction that can occur between them and improve stability characteristics. Therefore a higher gain in the inner loop can be adopted. An additional advantage is, that the plant nonlinearities are handled by the controller in the inner loop and they do not have meaningful influence on the outer loop [5].

In this paper the cascade control structure is proposed, as a solution to control task formulated as an angular stabilization. The angular velocities of the rotating platform are additional measurements that can be used in the inner loop. In this case, there is no need to assemble any extra sensors, thus the AHRS (Attitude and Heading Reference Signal) provides not only angels but also other raw data, such as accelerations, angular velocities and gravitational field strength. The outer loop is based on the Euler angels, the measurements are calculated from the combination of the accelerometers, gyroscopes and magnetometer. The cascade control loop for the quadrotor vehicle is shown in Fig. 4.

3.1 Inner and Outer PID controllers

In both loops three types of PID controllers are considered.

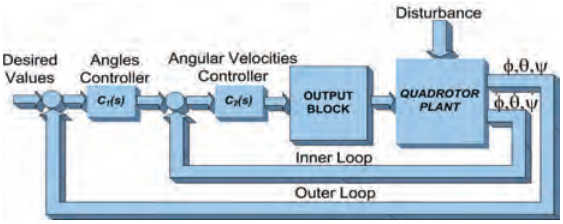

Figure 4: Cascade control system for quadrotor.

3.2 PID Controller – type A

In control theory the ideal PID controller in parallel structure is represented in the continuous time domain as follows:

$$u(t) = K_p e(t) + K_i \int_0^t e(\ )d \ + K_d \frac{de(t)}{dt} \tag{16}$$

where: K_p - proportional gain,

K_i - integral gain,

K_d - derivative gain.

A block diagram that illustrates given controller structure is shown in the Fig. 5.

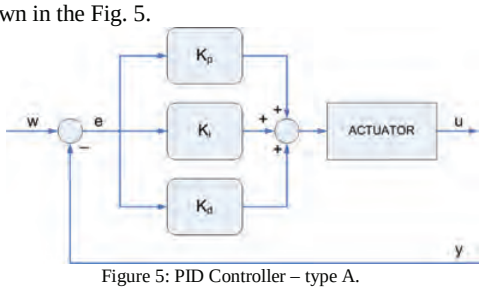

Figure 5: PID Controller – type A.

The problem with conventional PID controllers is their reaction to a step change in the input signal which produces an impulse function in the controller action. There are two sources of the violent controller reaction, the proportional term and derivative term. Therefore, there are two PID

http://www.imavs.org/

controller structures that can avoid this issue. In literature exists different names [2], [5]: type B and type C; derivative-of-output controller and set-point-on-I-only controller; PI-D and I-PD controllers. The main idea of the modified structures is to move either the derivative part or both derivative and proportional part from the main path to the feedback path. Therefore, they are not directly subjected by jump of set value, while their influence on the control reaction is preserved, since the change in set point will be still transferred by the remaining terms.

3.3 PID Controller – type B

It is more suitable in practical implementation to use "derivative of output controller form". The equation of type B controller is following:

$$u(t) = K_p e(t) + K_i \int_0^t e(\ )d\ - K_d \frac{dy(t)}{dt} \tag{17}$$

A block diagram that illustrates given controller structure is shown in Fig. 6.

If PI-D structure is used, discontinuity in r(t) will be still transferred through proportional into control signal, but it will not have so strong effect as if it was amplified by derivative element.

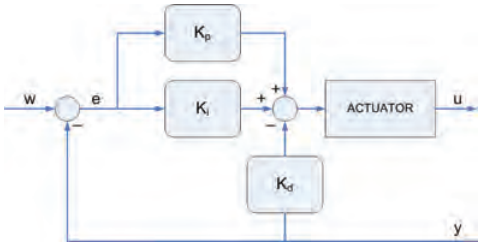

Figure 6: PID Controller – type B.

3.4 PID Controller – type C

This structure is not so often as PI-D structure, but it has certain advantages. Control law for this structure is given as:

$$u(t) = -K_p y(t) + K_i \int_0^t e(\ )d\ - K_d \frac{dy(t)}{dt} \tag{18}$$

Block diagram for type C controller is shown in Fig. 7.

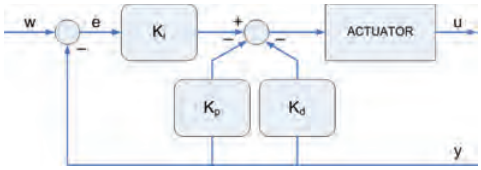

Figure 7: PID Controller – type C.

With this structure transfer of reference value discontinuities to control signal is completely avoided. Control signal has less sharp changes than with other structures.

4 SIMULATIONS RESULTS

In this section, we present the results of simulations which were conducted to evaluate the performance of the designed attitude control system in the cascade structure with different types of PID controllers. The presented simulations consisted in transition with predefined dynamics from one steady-state flight to another. In the design process we consider three types of PID controllers (type A, B, C) optimizing the parameters in view of the assumed reference model. To evaluate the quality of control it was taken into account the tracking of the reference model, and in particular the realizability of the control in practical aspects.

The entire MIMO control system consists of three cascade control channels with two PID controllers each of them. Feedback data for the regulators are six variables: Euler angles , , (outer loop) and angular velocities , , (inner loop). Control signals are motors inputs: u_1, u_2, u_3, u_4. The general control task is stated as a tracking problem for the following variables:

$$\begin{aligned} &\lim_{t\to\infty}\left[\ _0(t) - \ (t)\right] = 0 \\ &\lim_{t\to\infty}\left[\ _0(t) - \ (t)\right] = 0 \\ &\lim_{t\to\infty}\left[\ _0(t) - \ (t)\right] = 0 \end{aligned} \tag{19}$$

where $_0(t)$, $_0(t)$, $_0(t)$ are the desired values of the considered variables.

In view of the complexity and multidimensionality of the considered problem only the results in pitch control channel are presented.

The tuning of the cascade controller parameters were made in two steps. First, inner loop controller was tuned based on the assumed reference model. The desired dynamics is determined by a following transfer function:

$$K_{ref,1}(s) = \frac{1}{sT_I + 1} \tag{20}$$

where $T_I = 0.25\ [s]$.

At this stage of designing we consider three structures of PID controller: type A, type B (PI-D), and type C (I-PD).

In this case the accuracy requirements for the system are formulated in a form of two performance indices related to the time responses of the system. Therefore, there was introduced the following quadratic integral index for the tracking performance:

$$I_{tr} = \int_0^T \left[w(t) - y(t)\right]^2 dt \tag{21}$$

Second index determines the effort of control signal and is defined as follows:

$$I_U = \int_0^T u^2(t)\,dt \tag{22}$$

Numerical results are shown in Table 1.

Structure	Value
Control Index	
Type A	1399.365
Type B	1.8674
Type C	4.8704
Tracking Index	
Type A	0.90128
Type B	0.77048
Type C	1.0

Tabel1: Performance Indices.

http://www.imavs.org/

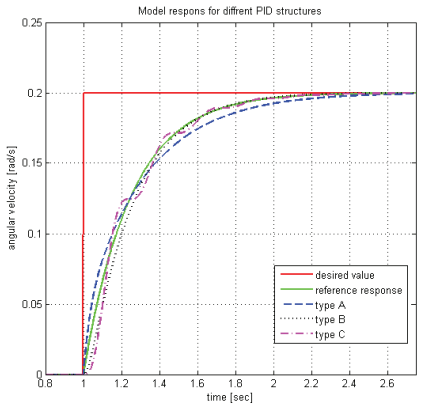

Figure 8:Time history of angular velocity .

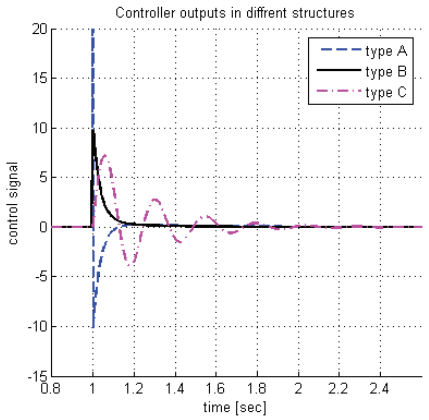

Figure 9:Time history of control signal u .

Remark 1: The relative order of the inner loop with PID controller is equal one.
Remark 2: Based on the remark 1 the reference model is provided by the first order inertia system (20).
Remark 3: Gradient descent method allows to tune the controller parameters, and obtain the satisfactory reference model tracking results in all structures (Table1).
Remark 4: However, the index of control signal effort in particular types of PID controllers indicates significant differences.
Remark 5: In the terms of practical implementation the type A seems to be not acceptable (value=2047). On the basis of the presented findings, the most common structure is type B, therefore this one will be used in the next step, as the best possible solution.

In the second step the outer loop controller was tuned based on the assumed following reference model:

$$K_{ref,O}(s) = \frac{1}{{}^{2}s^{2} + 2 \quad s + 1} \tag{23}$$

where: $= 0.4$ - undamped resonance period,
$= 1$ - relative damping factor.

Remark 6: In respect of the slower outer loop dynamics the reference model was determined as a second order differential equation (23).

Remark 7: Referring to remark no. 5, the advantages of the type B PID controller has been confirmed in cascade control system.

Remark 8: In case of PI controller the architectures type A and B are equivalent.

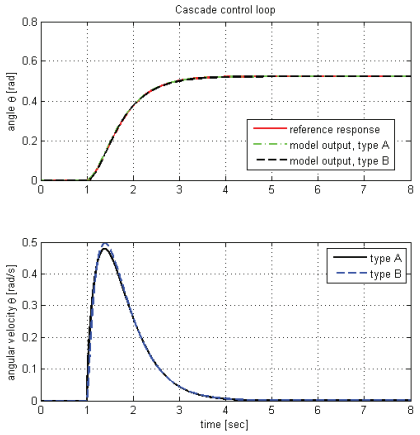

Figure 10:Time history of pitch angle and angular velocities.

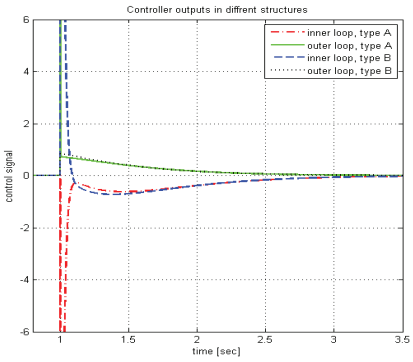

Figure 11: Controllers signals.

5 CONCLUSION

In this paper, the different approaches to the problem of attitude control of a quadrotor were considered. The main goal of this research is the evaluation of different types of PID algorithm in practical aspects of control systems design. Three architectures were presented and examined with respect to the best performance. All of the reviewed architectures of the controllers resulted in almost the same model output response time but significantly different control signals. Taking into consideration the proposed control effort index, type B architecture is the most comprehensive choice.

Assumed reference models provides time separation between fast and slow dynamics in the cascade system. The application of a cascade control structure gives the possibility to adapts the simple PID algorithm for controlling complex systems, such as vertical take-off and landing platform. Proposed approach is an alternative solution to the advanced control algorithms but it requires additional sensor, which provides measurement for the inner control loop. However, from the point of unmanned aerial vehicle,

such as quadrotor, the cascade control architecture can be implemented without any extra sensing elements.

The conducted simulations and analysis proved the ability, of the designed cascade structure, to control the orientation platform angles, and provide the promising fundamentals for practical experiments with a physical plant.

ACKNOWLEDGMENT

This work has been granted from funds for science in 2010-2012 as a development project No. OR00011811.

REFERENCES

[1] A. Tayebi and S. McGilvray, "Attitude stabilization of a VTOL quadrotor aircraft", *IEEE Trans. on Control Systems Technology*, vol. 14, no. 3, 2006, pp. 562-571.
[2] A. Visioli, "Practical PID Control", Springer-Verlag, London 2006
[3] H. Bouadi and M. Tadjine, "Nonlinear observer design and sliding mode control of four rotors helicopter", *Int. Jour. of Mathematical, Physical and Engineering Sciences*, vol. 1, no.2, pp. 115-120.
[4] H. Bouadi, M. Bouchoucha, and M. Tadjine, "Sliding mode control based on backstepping approach for an UAV type-Quadrotor", Int. Jour. of Applied Mathematics and Computer Sciences, vol. 4, no. 1, pp. 12-17.
[5] H. L. Wade, "Basic and Advanced Regulatory Control: System Design and application", ISA, United States of America, 2004.
[6] K. P. Valavanis, *Advances in Unmanned Aerial Vehicles.* The Netherlands: Springer-Verlag, 2007.
[7] K.Nonami, F. Kendoul, S. Suzuki, W. Wang, D. Nakzawa, 2010. *Autonomous Flying Robots.* Spirnger, 1st edition.
[8] P. Castillo, R. Lozano, and A. E. Dzul, *Modelling and Control of Mini-flying Machines.* London: Springer-Verlag, 2005, ch. 3.
[9] P. Lindahl, E. Moog and S.R. Shaw, 2009. *Simulation, Design and Validation of a UAV SOFC Propulsion System.* Aerospace Conference, pp.1-8, Big Sky, MT.
[10] R. Czyba, 2009. *Attitude Stabilization of an Indoor Quadrotor*. Proc. Of European Micro Aerial Vehicle Conference and Competition, EMAV.
[11] *R. Goel, S.M. Shah, N.K. Gupta, N. Ananthkrishnan, 2009.* Modeling, Simulation and Flight of an Autonomous Quadrotor. *Proceedings of ICEAE.*
[12] S. Bouabdallah, "Design and control of quadrotors with application to autonomous flying", Ph.D. dissertation, School of Computer and Communication Sciences, Lausanne, 2007.
[13] S. Bouabdallah, A. Noth, and R. Siegwart, "PID vs LQ control techniques applied to an indoor micro quadrotor", *Proc. of Int. Conf. On Intelligent Robots and Systems, Japan, 2004.*
[14] V. D. Yurkevich, *Design of Nonlinear Control Systems with the Highest Derivative in Feedback.* World Scientific Publishing, 2004.

http://www.imavs.org/